



Spatial and temporal distribution characteristics and risk assessment of heavy metals in groundwater of Pingshuo mining area

Long Sun · Tingxi Liu · Limin Duan · Xin Tong ·
Wenrui Zhang · He Cui · Zhiting Wang ·
Guofeng Zheng

Received: 11 September 2023 / Accepted: 8 February 2024 / Published online: 15 March 2024
© The Author(s), under exclusive licence to Springer Nature B.V. 2024

Abstract Groundwater pollution in the Pingshuo mining area is strongly associated with mining activities, with heavy metals (HMs) representing predominant pollutants. To obtain accurate information about the pollution status and health risks of groundwater, 189 groups of samples were collected from four types of groundwater, during three periods of the year, and analyzed for HMs. The results showed that the concentration of HMs in groundwater was higher near the open pit, waste slag pile, riverfront area, and human settlements. Except for Ordovician groundwater, excessive HMs were found in all investigated groundwater of the mining area, as compared with the standard thresholds. Fe exceeded the threshold in 13–75% of the groundwater samples. Three sources of HMs were identified and quantified by Pearson's correlation analysis and the PMF model, including coal mining activities (68.22%), industrial, agricultural, and

residential chemicals residue and leakage (16.91%), and natural sources (14.87%). The Nemerow pollution index revealed that 7.58% and 100% of Quaternary groundwater and mine water samples were polluted. The health risk index for HMs in groundwater showed that the non-carcinogenic health risk ranged from 0.18 to 0.42 for adults, indicating an acceptable level. Additionally, high carcinogenic risks were identified in Quaternary groundwater (95.45%), coal series groundwater (91.67%), and Ordovician groundwater (26.67%). Both carcinogenic and non-carcinogenic risks were greater for children than adults, highlighting their increased vulnerability to HMs in groundwater. This study provides a scientific foundation for managing groundwater quality and ensuring drinking water safety in mining areas.

Keywords Heavy metals · Groundwater · Mine water · Risk assessment · Source apportionment · Coal mining

Supplementary Information The online version contains supplementary material available at <https://doi.org/10.1007/s10653-024-01906-7>.

L. Sun · T. Liu (✉) · L. Duan · X. Tong · W. Zhang ·
He. Cui · Z. Wang · G. Zheng
College of Water Conservancy and Civil Engineering,
Inner Mongolia Agricultural University, Hohhot 010018,
China
e-mail: txliu1966@163.com

T. Liu · L. Duan · X. Tong
Inner Mongolia Key Laboratory of Water Resource
Protection and Utilization, Hohhot 010018, China

Introduction

Groundwater is a critical source of drinking water worldwide, which humans have extensively used throughout history, and this dependence continues to increase (Sun et al., 2022c). Groundwater quality and availability are the major contributor to human health and sustainable development (Cui et al., 2021). In recent decades, heavy metals (HMs) pollution in

groundwater has become a serious problem, due to its persistence, non-degradable nature, high toxicity, and enrichment in the human body (Sajjadi et al., 2022; Santana et al., 2020). Groundwater quality is highly susceptible to various anthropogenic activities, particularly, mining is responsible for releasing large amounts of HMs into the surrounding areas (Shi et al., 2022), which enters to the groundwater through eluviation, leaching, and osmosis (Sharma et al., 2022; Wang et al., 2019b).

Several studies have been conducted on environmental geochemistry of HMs in groundwater in the coal mining areas in some parts of the world. For instance, Kim et al. (2017) investigated geochemical behaviors of metals in groundwater in mine areas of South Korea. Wang et al. (2019b) studied the environmental geochemistry of heavy metals in the groundwater of coal mining areas. Qin et al. (2021) presented sources and migration of heavy metals in a karst water system under the threats of an abandoned Pb–Zn mine, in southwest China. Most of research work conducted to date on HMs of groundwater in mining areas are restricted to a single mine or to a specific type of groundwater or mixed groundwater. Therefore, there are still a limited number of comprehensive studies on distribution, sources, and health risk assessment of HMs in the various types of groundwater in coal mining areas. Furthermore, groundwater contaminated by HMs in coal mining areas could pose a serious long-term threat to the surrounding environment. Therefore, finding out the spatiotemporal distribution characteristics of HMs in groundwater in the coal mining area, analyzing the sources of HMs pollution, and then evaluating the risks to human body are of great practical significance for ensuring the safety of drinking water and HMs pollution control.

It has been reported that the main sources of HMs in groundwater include natural and human factors (Jiang et al., 2021a; Kaur et al., 2020; Sheng et al., 2022). Quantitative identification of potential sources of HMs in groundwater is essential to pollution control and reduction (Sheng et al., 2022). In recent years, the positive matrix factorization (PMF) model has been widely applied to identify and quantify the origins of HMs in groundwater (Huang et al., 2021), based on its obvious advantages of accurately modeling all data (Haghnazar et al., 2022), and making sources more physically reliable (Sheng et al.,

2022). The high concentration of HMs in groundwater not only affects the environment but also threatens human health. Previous studies found that HMs can cause significant long-term risks to human health via dermal absorption and ingestion (Jiang et al., 2021a; Wang et al., 2021). Cd, Cr, As, Pb, and Hg are highly toxic to the human body, even at low concentrations (Xiao et al., 2021). Fe, Mn, Ni, Zn, and Se are necessary for the normal function of the human body, whereas their excessive intake can be detrimental to human health (Ali et al., 2013; Singh & Kumar, 2017). Heavy metal risk assessment is a considerable part of environmental risk assessment, including pollution and health risk assessments. Among them, the Nemerow pollution index method has been generally adopted to comprehensively evaluate the pollution level of groundwater (Mukherjee et al., 2020). This approach considers individual factors' maximum and average values, emphasizing the effect of main pollutants (Li et al., 2022). The typical health risk assessment model is commonly utilized to assess health risks to human body, including the non-cancer and cancer risks, according to the actual concentration of HMs in groundwater (Gu et al., 2020; Sajjadi et al., 2022; Wang et al., 2021). The composition and origin of HMs in different types of groundwater vary, and different HMs have different toxicities (Sheng et al., 2022). Furthermore, under the combined disturbance of open-pit and underground coal mining, more frequent and complex changes in the concentration and distribution characteristics of HMs occur in groundwater (Zhang et al., 2019). Thus, an integrated assessment method, combining the PMF model, Nemerow pollution index, and health risk assessment, was applied in this research.

The Pingshuo mining area is one of the main coal mining bases in north China, and the groundwater is an important water source for drinking, industrial application, and agricultural production. Groundwater pollution by HMs in the basin is becoming increasingly prominent (Yan et al., 2020). Groundwater pollution affects the health of children and adults in this area. Given the above, the HMs pollution characteristics and comprehensive health risk assessment were conducted for four types of groundwater (Quaternary groundwater, coal series groundwater, Ordovician groundwater, and mine water) in this area. The main objectives of this work were: (1) to explore the spatiotemporal distribution characteristics of HMs in

different types of groundwater; (2) to investigate possible sources of HMs using PMF model; and (3) to assess the pollution and health risks of different types of groundwater and ascertain the dominant pollution elements of the groundwater. This study provides a scientific basis for groundwater quality risk management, development and protection of water resources, and the safety of drinking water and the ecological environment in the Pingshuo mining area.

Materials and methods

Study area

The Pingshuo mining area (112°12'–112°31' E, 39°23'–39°35' N) is located at the north end of Ningwu coalfield in the northwest of Shanxi province, Northern China (Fig. 1), covering an area of 320 km². The area is characterized by a typical north temperate, semiarid, continental monsoon climate, characterized by rare rainfall and strong evaporation. The average annual temperature, rainfall, and evaporation are 7.3 °C, 420.1 mm, and 1853.3 mm (Φ20 cm pan), respectively. Data on average monthly precipitation, evaporation, and temperature between 1957 and 2020 in Shuozhou city are shown in Fig. S1.

According to the historical hydrological data of the study area, the year is subdivided into three periods, including the high, stable, and low-water periods. The high-water period is from June to September, while April, May, October, and November are considered as the stable-water period. The low-water period is from December to March. The northern, western, and eastern terrain of the study area is high, while the central part involves hills, which belong to the typical loess plateau landform type, with an elevation of 1107–2141 m above mean sea level (Fig. 1). The strata in the study area contain Ordovician, Carboniferous, and Permian as the geological base, and their lithology is mainly gray thick layered limestone, mudstone, and gray blue gray medium coarse–coarse sandstone, respectively. The Tertiary brown, red clay, and the Quaternary light-yellow sandy soil and loess are usually found on the surface. The mineral types in the study area are mainly coal resources. Coal-bearing strata are the Permian Shanxi Formation and the Carboniferous Taiyuan Formation. The main potentially exploitable coal seams (No. 4 and 9) are present in the Taiyuan Formation of Carboniferous. This area has three open-pit coal mines and nineteen underground coal mines, producing 100 million tons of raw coal per year. According to the types of aquifer media, occurrence conditions, and hydrodynamic

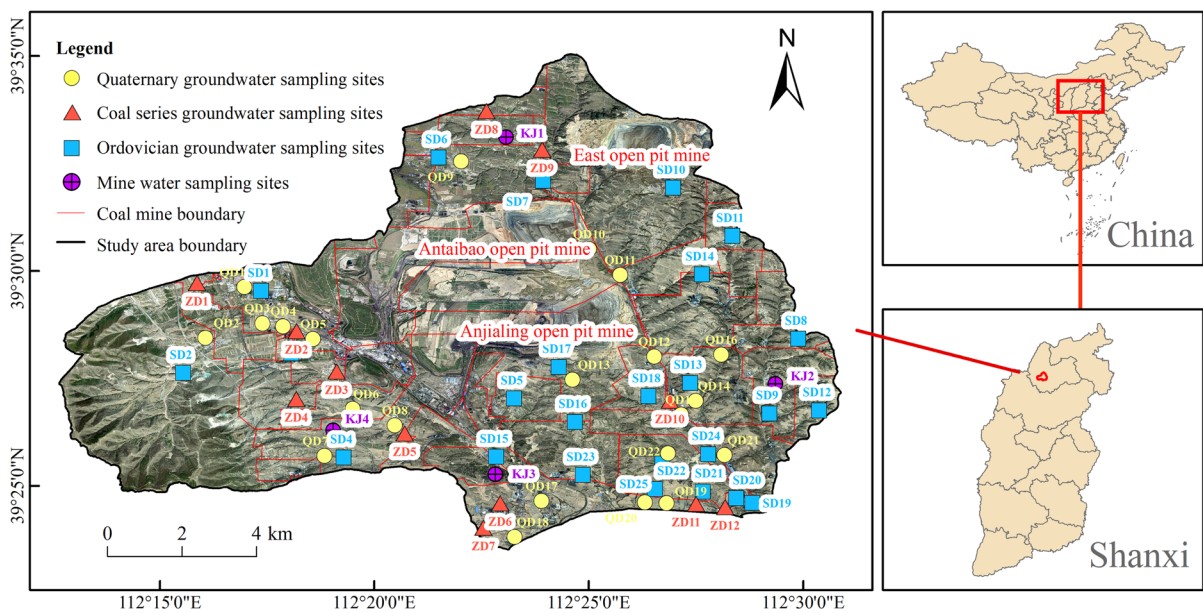


Fig. 1 Maps of study and sampling sites

characteristics, the groundwater in the study area includes Quaternary groundwater, coal series groundwater, and Ordovician groundwater. The Quaternary groundwater mainly occurs in the Quaternary aquifer, with aquifer floor buried depth of < 100 m and thickness of 3–50 m, reflecting better water abundance, with water level depth of 5–50 m. The underlying Tertiary aquifuge separates Quaternary groundwater from the coal series aquifer, and Tertiary strata have discontinuous distribution in this area. The coal series groundwater is mainly present in the Upper and Lower Shihezi Formation of Permian, Shanxi Formation, and Carboniferous Taiyuan Formation, with an aquifer floor depth of 100–380 m, thickness of 50–70 m, with a lower water abundance, and a water level depth of > 50 m. The underlying Carboniferous Benxi Formation mudstone effectively separates coal series groundwater from the Ordovician limestone aquifer, and having a better barrier effect. The Ordovician groundwater occurs in the Ordovician limestone with better water abundance and a water level depth of 200 m, representing the main water supply source in the study area. The groundwater runoff conditions in the study area are good, with runoff from northwest to southeast.

Sample collection and analysis

Groundwater samples were collected in July 2020, October 2020, and January 2021, representing the high-, stable-, and low-water periods, respectively. A total of 189 groups of groundwater samples were taken, including 66 groups of Quaternary groundwater, 36 groups of coal series groundwater, 75 groups of Ordovician groundwater, and 12 groups of mine water. Each group contained three parallel groundwater samples. The sampling locations are shown in Fig. 1. A specifically designed, self-made sampler was used to collect groundwater with a buried depth < 15 m. The sampler was sunk 2 m below the water surface, and held for 1–2 min on the same position, to ensure representative water samples. The groundwater with a buried depth > 15 m was sampled by water pump. The water was pumped for 3 min, and then the water pH was monitored every 15 s. The samples were collected after getting stable pH (± 0.1 variation) for three continuous readings. The collected water samples were filtered through a 0.45- μm pore size membrane, and immediately transferred into pre-cleaned 200-mL high density

polyethylene bottles. Few drops of high-grade pure nitric acid were added to keep the $\text{pH} < 2$, and capped with the sealing film produced by Parafilm Company of the USA to avoid air contact and evaporation. The samples were transported to the laboratory in the incubator. In the laboratory, the water samples were stored in refrigerator at 4 °C until analysis. The pH of each groundwater sample was monitored in situ and recorded by the portable multi-parameter instrument (Aqua TROLL 400). Concentrations of nine typical HMs in groundwater samples including Cr, Mn, Fe, Ni, Cu, Zn, As, Cd, and Pb were determined by inductively coupled plasma–mass spectrometry method (ICP–MS, Thermo Fisher, USA). For quality assurance and quality control, before conducting the on-machine testing, the collected samples were filtered using a 0.22- μm membrane filter into the sample vial for subsequent analysis. The standard curves with concentration gradients of 1, 2, 5, 10, 20, 50, and 100 $\mu\text{g/L}$ were prepared using the multi-element standard solution produced by China National Standard Research Center. Blank samples of deionized water, sample duplicates, and recovery rate tests were performed during sample analysis. The relative standard deviations of the duplicate samples were < 5% and the recovery rate ranged from 85 to 112% of each calibration element.

Source apportionment model

The PMF model, recommended by USEPA, is a multivariate factor analysis tool (Haghnazar et al., 2022), widely applied to identify and quantify the origins of HMs in groundwater by accurately modeling all data (Huang et al., 2021). The core of the algorithms for the PMF model is to make the objective function (Q) values small and stable (Yoon et al., 2023). According to the PMF 5.0 user manual, the basic equations are as shown below:

$$x_{ij} = \sum_{k=1}^p g_{ik} f_{kj} + e_{ij} \quad (1)$$

$$Q = \sum_{i=1}^n \sum_{j=1}^m \left(\frac{e_{ij}}{u_{ij}} \right)^2 \quad (2)$$

$$u_{ij} = \begin{cases} \frac{5}{6} \times \text{MDL}, & C \leq \text{MDL} \\ \sqrt{(\delta \times C)^2 + \text{MDL}^2}, & C > \text{MDL} \end{cases} \quad (3)$$

where i, j , and k are the number of samples, elements, and different sources, respectively; x_{ij} is the concentration of element j in sample i ; p is the total number of sources; n is the total number of samples, m is the total number of elements; g is the contribution rate; f is the source curve; Q is the objective function; e is the residual; u is uncertainty; δ is the error rate, and δ is set at 15%; C is the measured value of element concentration; MDL is the method detection limit, which was calculated using the raw intensity data of the standard and the blank. The MDLs of Cr, Mn, Fe, Ni, Cu, Zn, As, Cd, and Pb are 0.020, 0.002, 4.500, 0.006, 0.009, 0.069, 0.004, 0.003, and 0.002 $\mu\text{g/L}$, respectively.

The relative contributions of the factors for each sample were calculated using the following equation:

$$C_i = \frac{F_i}{\sum_{i=1}^n F_i} \quad (4)$$

where C_i and F_i are the relative and absolute contributions of factor i , respectively, and n is the total number of factors.

Risk assessment approaches

Nemerow pollution index

The Nemerow pollution index is a comprehensive method for assessment of HMs pollution levels in groundwater, based on a simple and straightforward mathematical model (Mukherjee et al., 2020). The equations used for the calculation are as follows (Bodrud-Doza et al., 2019; Egbueri & Unigwe, 2020):

$$P_i = \frac{C_i}{S_i} \quad (5)$$

$$PI_N = \sqrt{\frac{P_{i\max}^2 + P_{i\text{ave}}^2}{2}} \quad (6)$$

where P_i is the single pollution index of HMi , C_i is the measured concentration of HMi , and S_i represents the groundwater quality standard concentration of

HMi ; PI_N is the Nemerow pollution index of the n th sample point, $P_{i\max}$ is the maximum value of the single pollution index of all the HMs in the n th sample point, and $P_{i\text{ave}}$ is the average value of the single pollution index of all the HMs in the n th sample point. The interpretation of PI_N was as follows: no pollution ($PI_N < 0.5$), clean (0.5–0.7), warn (0.7–1.0), mild pollution (1.0–2.0), moderate pollution (2.0–3.0), and heavy pollution ($PI_N > 3$) (Haque et al., 2020).

Health risk assessment

The nine HMs tested in this study were divided into carcinogenic (Cr, As, and Cd) and non-carcinogenic (Mn, Fe, Ni, Cu, Zn, and Pb) metal elements. As prescribed by the USEPA, the health risk assessment model was applied to evaluate the health risks of adults and children through ingestion and dermal absorption (Giri & Singh, 2014; Wen et al., 2019). The specific calculation steps were as follows:

(1) Chronic daily intake (CDI).

The USEPA computes CDI from the amount of a particular HM element in groundwater absorbed by the human body through direct ingestion and dermal absorption, using the following mathematical equations (Qu et al., 2018).

$$CDI_{\text{ingestion}} = \frac{C_i \times IR \times EF \times ED}{BW \times AT} \quad (7)$$

$$CDI_{\text{dermal}} = \frac{C_i \times SA \times K_p \times ET \times EF \times ED \times CF}{BW \times AT} \quad (8)$$

$CDI_{\text{ingestion}}$ and CDI_{dermal} indicate the chronic daily intake from water ingestion and dermal absorption ($\mu\text{g/kg/day}$), respectively, and C_i is the average concentration of a certain HM in water ($\mu\text{g/L}$). IR is the ingestion rate (2.2 L/d for adults, and 1.14 L/d for children), EF is the exposure frequency (365 days/year), and ED is the exposure duration (70 years for adults, and 9 years for children). BW is the body weight (64 kg for adults and 25 kg for children in Shanxi Province; Xie et al., 2021), AT is the average time ($ED \times 365$ days/year, i.e., 25,550 days for adults and 3285 days for children), SA is the exposed skin area (17,000 cm^2 for adults, and 8000 cm^2 for children), K_p (cm/h) is the dermal permeability coefficient of the metals in water (Table S1), ET is the exposure time (0.58 h/day for adults, and 1 h/day for

children; Shil & Singh, 2019), and CF is the transfer factor (1×10^{-3} mL/cm³) for water.

(2) Non-carcinogenic health hazards assessment.

In this study, the hazard quotient (HQ) and hazard index (HI) were used to estimate the non-carcinogenic health risk of HMs in groundwater (Cui et al., 2021). The equations used for calculation of HQ and HI are presented below:

$$HQ_{\text{ingestion}} = \frac{ADD_{\text{ingestion}}}{RfD_{\text{ingestion}}} \text{ or } HQ_{\text{dermal}} = \frac{ADD_{\text{dermal}}}{RfD_{\text{dermal}}} \quad (9)$$

$$HI = \sum (HQ_{\text{ingestion}} + HQ_{\text{dermal}}) \quad (10)$$

where $HQ_{\text{ingestion}}$ and HQ_{dermal} are the hazards quotient of ingestion and dermal, respectively. $RfD_{\text{ingestion}}$ and RfD_{dermal} are the chronic reference doses of ingestion and dermal ($\mu\text{g}/\text{kg}/\text{day}$), respectively. The USEPA reference values of $RfD_{\text{ingestion}}$ and RfD_{dermal} for an individual HMs are shown in Table S1. According to USEPA classification, HQ and $HI < 1$ indicate an acceptable non-carcinogenic risk, where the risk of non-carcinogenic effects increases with an increase in HQ and HI values, while the values > 1 indicate a higher probability of adverse health effects (Cui et al., 2021).

(3) Carcinogenic health risk assessment.

The carcinogenic health risk of HMs in groundwater was estimated using the incremental lifetime cancer risk (ILCR) model of USEPA.

$$\begin{aligned} ILCR_{\text{ingestion}} &= ADD_{\text{ingestion}} \times SF_{\text{ingestion}} \text{ or } ILCR_{\text{dermal}} \\ &= ADD_{\text{dermal}} \times SF_{\text{dermal}} \end{aligned} \quad (11)$$

$$ILCR = \sum (ILCR_{\text{ingestion}} + ILCR_{\text{dermal}}) \quad (12)$$

where $ILCR_{\text{ingestion}}$ and $ILCR_{\text{dermal}}$ indicate the ILCR of ingestion and dermal. $SF_{\text{ingestion}}$ and SF_{dermal} denote the cancer slope factor of ingestion and dermal ($\text{kg}/\text{d}/\mu\text{g}$), respectively. The USEPA values of $SF_{\text{ingestion}}$ and SF_{dermal} for individual HMs are shown in Table S1. According to USEPA, a ILCR value $< 10^{-6}$ represents negligible levels, values $10^{-6} < ILCR < 10^{-4}$ indicate acceptable levels, while $ILCR > 10^{-4}$ shows a high cancer risk to humans (Li et al., 2022). The values for other parameters (Giri & Singh, 2014; Miguel et al., 2007; Wang et al., 2017) in the model are shown in Table S1.

Results and discussion

The concentrations and temporal distribution characteristics of HMs in groundwater

The HMs concentrations and pH values of groundwater in the Pingshuo mining area are presented in Table 1. The pH value of the groundwater varied from 7.02 to 8.81, showing that the groundwater was weakly alkaline. In general, the average concentrations of HMs in the Quaternary groundwater were in the following order $\text{Fe} > \text{Zn} > \text{Mn} > \text{Cr} > \text{Ni} > \text{Pb} > \text{Cu} > \text{As} > \text{Cd}$, whereas in coal series groundwater the order was $\text{Fe} > \text{Mn} > \text{Zn} > \text{Cr} > \text{Ni} > \text{Cu} > \text{Pb} > \text{As} > \text{Cd}$, in Ordovician groundwater $\text{Fe} > \text{Zn} > \text{Mn} > \text{Cr} > \text{Ni} > \text{Cu} > \text{Pb} > \text{Cd} > \text{As}$, and in mine water $\text{Fe} > \text{Mn} > \text{Zn} > \text{Ni} > \text{Cu} > \text{Pb} > \text{Cr} > \text{As} > \text{Cd}$. These results suggested the existence of some differences in the order of average values of these HMs in groundwater samples, which may be due to the close relationship between the concentration of trace elements in groundwater and its hydrogeological conditions (Wang et al., 2016). Fe, Mn, and Zn were identified as the top three abundant elements in each type of groundwater, reflecting contamination from exploitation of coal resources (Jiang et al., 2021a). The concentration of Cd was higher than As in Ordovician groundwater, while the opposite result was found in other types of groundwater, which suggested that the increase of As concentration was closely associated with the occurrence and exploitation of coal resources and anthropic production (Jiang et al., 2021a). The concentration of Pb in the Quaternary groundwater was higher than that of Cu, while the opposite result was observed in other types of groundwater. As is generally known as the source of Pb in groundwater mainly caused by mineral dissolution or man-made pollution. In this study, the possibility that the Pb came from dissolved minerals was excluded according to the geological composition. Therefore, the Pb enrichment in groundwater is mainly due to the equipment emissions and chemical residues originating from industrial, agricultural, and domestic activities. Pb enters the Quaternary groundwater through leaching and infiltration (Zheng & Bennett, 2002). Notably, the average concentrations of Fe (702.61 $\mu\text{g}/\text{L}$), Mn (325.77 $\mu\text{g}/\text{L}$), Ni (18.64 $\mu\text{g}/\text{L}$), and Cu (7.09 $\mu\text{g}/\text{L}$) in mine water were 3.85–5.43, 10.66–68.58, 9.14–13.51, and 4.25–5.41 times higher

Table 1 Descriptive statistics of HMs concentrations and pH of different types of groundwater

Types	Items	Cr µg/L	Mn µg/L	Fe µg/L	Ni µg/L	Cu µg/L	Zn µg/L	As µg/L	Cd µg/L	Pb µg/L	pH
Quaternary groundwater	Minimum	2.15	0.43	5.18	0.12	0.14	7.18	0.11	0.13	0.17	7.29
	Maximum	62.98	103.15	659.52	5.78	4.59	41.73	4.10	0.85	6.04	8.71
	Standard deviation	8.64	24.06	144.20	1.56	1.01	8.58	0.88	0.14	1.44	0.31
	Coefficient of variation	1.00	1.43	0.84	0.81	0.60	0.38	0.62	0.34	0.79	0.04
	Mean	8.64	16.81	171.53	1.93	1.67	22.42	1.43	0.41	1.82	7.97
	High-water period mean	6.04	15.32	191.97	2.02	1.26	27.32	1.18	0.41	1.71	7.95
	Stable-water period mean	9.28	14.16	137.50	1.84	2.05	19.70	1.49	0.40	1.82	7.92
	Low-water period mean	10.59	20.94	185.13	1.94	1.69	20.25	1.61	0.42	1.93	8.05
	Minimum	2.63	11.06	38.62	0.34	0.18	8.49	0.27	0.21	0.22	7.38
	Maximum	16.40	52.86	386.40	5.52	4.38	50.89	3.40	0.93	4.14	8.57
Coal series groundwater	Standard deviation	3.37	10.14	89.39	1.32	1.07	9.00	0.77	0.13	1.09	0.33
	Coefficient of variation	0.42	0.33	0.49	0.65	0.66	0.36	0.69	0.30	0.71	0.04
	Mean	8.05	30.55	182.51	2.04	1.63	25.07	1.12	0.43	1.53	8.01
	High-water period mean	5.84	32.67	225.08	2.50	1.62	27.41	1.22	0.41	1.50	7.93
	Stable-water period mean	8.69	28.65	132.10	2.03	2.00	22.44	1.08	0.44	1.64	8.00
	Low-water period mean	9.63	30.33	190.36	1.60	1.27	25.37	1.06	0.43	1.44	8.10
	Minimum	2.24	1.18	12.62	0.17	0.16	3.06	0.10	0.21	0.22	7.35
	Maximum	8.46	10.25	288.52	3.23	3.66	60.43	0.67	0.69	1.94	8.81
	Standard deviation	1.01	2.15	74.64	0.77	0.82	11.92	0.11	0.11	0.48	0.28
	Coefficient of variation	0.25	0.45	0.62	0.56	0.63	0.49	0.31	0.26	0.63	0.04
Ordovician groundwater	Mean	4.10	4.75	120.49	1.38	1.31	24.28	0.36	0.43	0.76	7.93
	High-water period mean	3.88	4.26	113.96	1.33	1.36	22.21	0.28	0.42	0.75	7.88
	Stable-water period mean	4.22	4.47	119.09	1.63	1.17	25.72	0.38	0.42	0.75	7.89
	Low-water period mean	4.22	5.52	128.41	1.18	1.38	24.92	0.42	0.44	0.78	8.03
	Minimum	0.24	206.54	109.53	3.65	1.09	14.16	0.14	0.25	0.28	7.47
	Maximum	7.05	385.85	1653.43	30.92	54.21	139.18	5.17	0.99	21.30	8.20
	Standard deviation	2.54	61.85	598.82	8.43	14.87	33.45	1.41	0.19	5.94	0.23
	Coefficient of variation	0.63	0.19	0.85	0.45	2.10	0.77	0.68	0.41	1.26	0.03
	Mean	4.06	325.77	702.61	18.64	7.09	43.27	2.06	0.46	4.72	7.91
	High-water period mean	2.52	322.14	457.99	16.15	2.51	33.64	1.50	0.42	0.54	8.03
Mine water	Stable-water period mean	6.69	326.34	759.22	20.92	3.14	32.09	2.79	0.41	3.77	7.86
	Low-water period mean	2.97	328.81	890.63	18.86	15.61	64.07	1.90	0.56	9.87	7.84
	Minimum	100	300	20	1000	1000	10	5	10	6.5–8.5	
	Maximum										
	Standard deviation										
	Coefficient of variation										
	Mean										
	High-water period mean										
	Stable-water period mean										
	Low-water period mean										
Chinese national standards ^a	50										

Table 1 (continued)

Types	Items	Cr $\mu\text{g/L}$	Mn $\mu\text{g/L}$	Fe $\mu\text{g/L}$	Ni $\mu\text{g/L}$	Cu $\mu\text{g/L}$	Zn $\mu\text{g/L}$	As $\mu\text{g/L}$	Cd $\mu\text{g/L}$	Pb $\mu\text{g/L}$	pH
WHO Guideline value ^b	50	400	300	70	2000	3000	10	3	10	6.5–9.5	

Coefficient of variation and pH no units

^aThe class III concentration threshold of the Chinese Groundwater Quality Standard (GB/T 14848–2017, 2017)

^bGuidelines for drinking-water quality

than of other types of groundwater. The high concentration of these HMs in mine water can be related to coal mining activities (Guo et al., 2022).

The coefficient of variation usually measures the dispersion of the test indicators in the samples. The higher coefficient of variation indicates a higher degree of dispersion and a more uneven spatial distribution (Wang et al., 2020). The coefficient of variation >0.5 indicates high variability (Liu et al., 2018). Based on the statistical analysis results, under the influence of human activities such as coal mining, and industrial and agricultural production, the spatial and temporal distributions of HMs in each type of groundwater were substantially different and showed high spatial variability. The coefficients of variation were >0.5 in seven elements (Mn, Cr, Fe, Ni, Pb, As, and Cu) of Quaternary groundwater, six elements (Cu, Pb, Fe, Zn, As, and Cr) of mine water, four elements (Pb, As, Cu, and Ni) of coal series groundwater and four elements (Pb, Cu, Fe, and Ni) of Ordovician groundwater. This may be due to the relatively high concentrations of HMs in some sampling sites and point source pollution. The pollution sources and pollution pathways of different HMs were inconsistent. In addition, the coefficient of variation of Mn and Cr in Quaternary groundwater was >1 , indicating that the Quaternary groundwater was more seriously affected by anthropogenic activities. A relatively lower (0.26–0.41) coefficient of variation for Cd was found in different types of groundwater, indicating stable Cd distribution. This is because Cd is greatly affected by geochemical background values and less by human activities, which is consistent the findings of Xie et al. (2021). The high concentrations of Fe, Ni, and Zn in the Quaternary groundwater were recorded in the high-water period, while high concentrations of other elements were mostly recorded in the low-water period. In the coal series groundwater, the high concentration of Cr was recorded in the low-water period, and the high value of other HMs was recorded in the high- and stable-water period. The high concentrations of Ni and Zn in the Ordovician groundwater were present in the stable-water period, and those of other elements were present in the low-water period. These results suggest that the atmospheric precipitation had a dilutive role in the Quaternary and Ordovician groundwater (Mahapatra et al., 2020), and the coal series groundwater was replenished by water with a high concentration of HMs in

the high- and stable-water period, demonstrating that atmospheric precipitation enhanced the release of HMs from the occurrence strata to the groundwater. The high concentrations of Cr, Ni, and As in mine water appeared in the stable-water period, and the high concentrations of other elements appeared in the low-water period. In this study, the sampling of the stable-water period and the low-water period was in autumn and winter. It is well known that the increase in coal production is due to the increase in coal demand in winter, which resulted in an increase in concentration of the HMs in mine water. Except Zn and As, the seasonal variation pattern of other HMs in mine water was parallel with that of Ordovician groundwater, which is probably because the Ordovician groundwater was the primary origin of mine water (Sun et al., 2022a).

By comparing the thresholds of the HMs set in Class III of the GB/T 14848–2017 and the guidelines for drinking-water quality issued by the World Health Organization (WHO), it was found that the Chinese Groundwater Quality Standard (GB/T 14848–2017) gives more stringent thresholds for HMs. Therefore, in this study, groundwater quality was assessed by the criterion of GB/T 14848–2017. In the Quaternary groundwater, the concentration of Cr (1.52%) exceeded the corresponding Class III threshold, and its maximum concentration was 1.26 times of the threshold. The concentrations of Mn surpassed the threshold in 4.55% and 100% of the samples of Quaternary groundwater and mine water, and the maximum recorded Mn concentrations for the two types of groundwater were 1.03 and 3.86 times higher than the threshold, respectively. The concentration of Fe in Quaternary groundwater, coal series groundwater, and mine water exceeded the threshold in 21.21, 13.89, and 75% of the samples, respectively, and its maximum concentration in the waters mentioned above was 2.20, 1.29, and five times the threshold, respectively. For mine water, the concentrations of Ni and Pb surpassed the threshold in 58.33 and 8.33% of the samples, and their maximum concentrations were 1.55 and 2.33 times the threshold, respectively. The concentrations of Cu, Zn, As, and Cd in the groundwater were all under the corresponding thresholds.

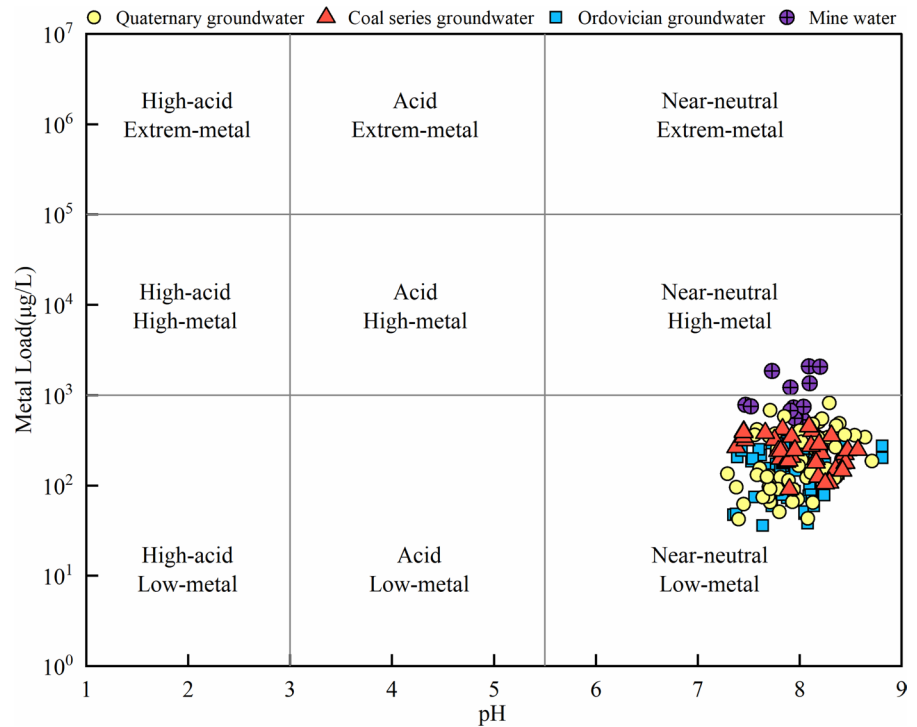
The method of Caboi & Cidu (1999) was adopted, using the metal load and water pH values, to classify the findings of these water samples. The Caboi diagram (Fig. 2) shows the degree of transfer of HMs,

which is in proportion to any difference in pH (Khan et al., 2021). In the present study, the metal load was calculated from the sum of the nine measured HMs. The samples, excluding mine water, were categorized as “near-neutral and low-metal.” However, 41.67% of mine water samples showed a “near-neutral and high-metal” classification, whereas 58.33% were in the near-neutral and low-metal concentration zone, which could be explained by coal mining, increasing the concentration of HMs in mine water (Guo et al., 2022).

Spatial distribution of HMs

Figure 3 shows spatial distribution of HMs concentrations in various types of groundwater. The high concentration of Cr in Quaternary groundwater was recorded near the east and south parts of the research area, and the high concentration of Cr in coal series groundwater occurred in the middle and south parts of the research area (ZD5 and ZD12), as shown in Figs. 1 and 3. These areas are places where human gathering. The concentration of Cr in almost all Ordovician groundwater samples was <5 $\mu\text{g/L}$. These findings clearly show that the source of Cr in groundwater was strongly linked to human activities (Jiang et al., 2021a), and there was a hydraulic relationship between Quaternary groundwater and coal series groundwater. The high level of Mn in Quaternary groundwater was present in riverside areas downstream or near open pits in the study area. The Mn concentrations of coal series groundwater were relatively high, ranging from 20 to 50 $\mu\text{g/L}$, and the spatial differences were not large. The concentration of Mn in Ordovician groundwater was <10 $\mu\text{g/L}$. These findings suggested that the changes in Mn concentration were greatly affected by the exploitation and occurrence of coal. The distribution characteristics of Fe and Ni were similar to those of Mn but also showed increases in human settlements, which suggested that Fe and Ni concentrations are also affected by other human activities. Cu and Zn concentrations in groundwater in the research area were 0.45–3.03 $\mu\text{g/L}$ and 12.75–46.39 $\mu\text{g/L}$, respectively, which were much lower than the standard limits (1000 $\mu\text{g/L}$), demonstrating their nonsignificant effect on human production. In Quaternary groundwater and coal series groundwater, a higher concentration of As was observed downstream compared to

Fig. 2 Caboi diagram showing metal load (Cr + Mn + Fe + Ni + Cu + Zn + As + Cd + Pb) versus pH plot



the upper stream of the study area, and markedly high values were recorded in a localized area (QD20 and ZD4), due to human pollution. In Ordovician groundwater, the concentration of As was $<0.82 \mu\text{g/L}$ with no distinct spatial variation.

The spatial distribution of Cd in each aquifer slightly differed, mostly in 0.25 to $0.5 \mu\text{g/L}$ range, with only few points exceeding $0.5 \mu\text{g/L}$, which may be related to the source of Cd in groundwater and the hydrogeochemistry of the environment in the study area. The high local concentration was due to anthropogenic activities such as coal mining. Wang et al. (2021) found that industrial pollution led to point source pollution of Cd in groundwater. The high concentration of Pb in Quaternary groundwater was observed in areas (QD15 and QD22) with serious human pollution. The spatial variation of Pb in coal series groundwater was not large, and the recharge of upper Quaternary groundwater mainly caused the increase in a localized area. The higher value of Pb concentration was observed in the middle of the research area in Ordovician groundwater. Multiple coal mining operations in this area have damaged the middle rock strata, and the formation of water-conducting fissures made the Ordovician groundwater

to directly recharge from the upper groundwater (Sun et al., 2022a).

The concentrations of Cr, Ni, and As from the first sampling site of mine water (KJ1) were higher than other sites, whereas the concentration of Fe from the second sampling site of mine water (KJ2) was higher than other sites, and those of Mn, Cu, Zn, Cd, and Pb from the fourth sampling site of mine water (KJ4) were higher than other sites, which might be due to the scale of coal mining. The mining scale of KJ4 was 10 million t/a, being much larger than that of KJ1 and KJ2, while KJ3 was in a state of shutdown. The high Fe concentration of KJ2 may be related to the strata occurred source water and the Fe-rich coal seam. Therefore, the spatial distribution of mine water was more complicated due to the complex sources and influence of human activities.

Source apportionment of HMs in groundwater

Correlation analysis

Different statistical analysis methods can be used to discriminate the relationship and source of HMs in water from a macroscopic point of view, to improve

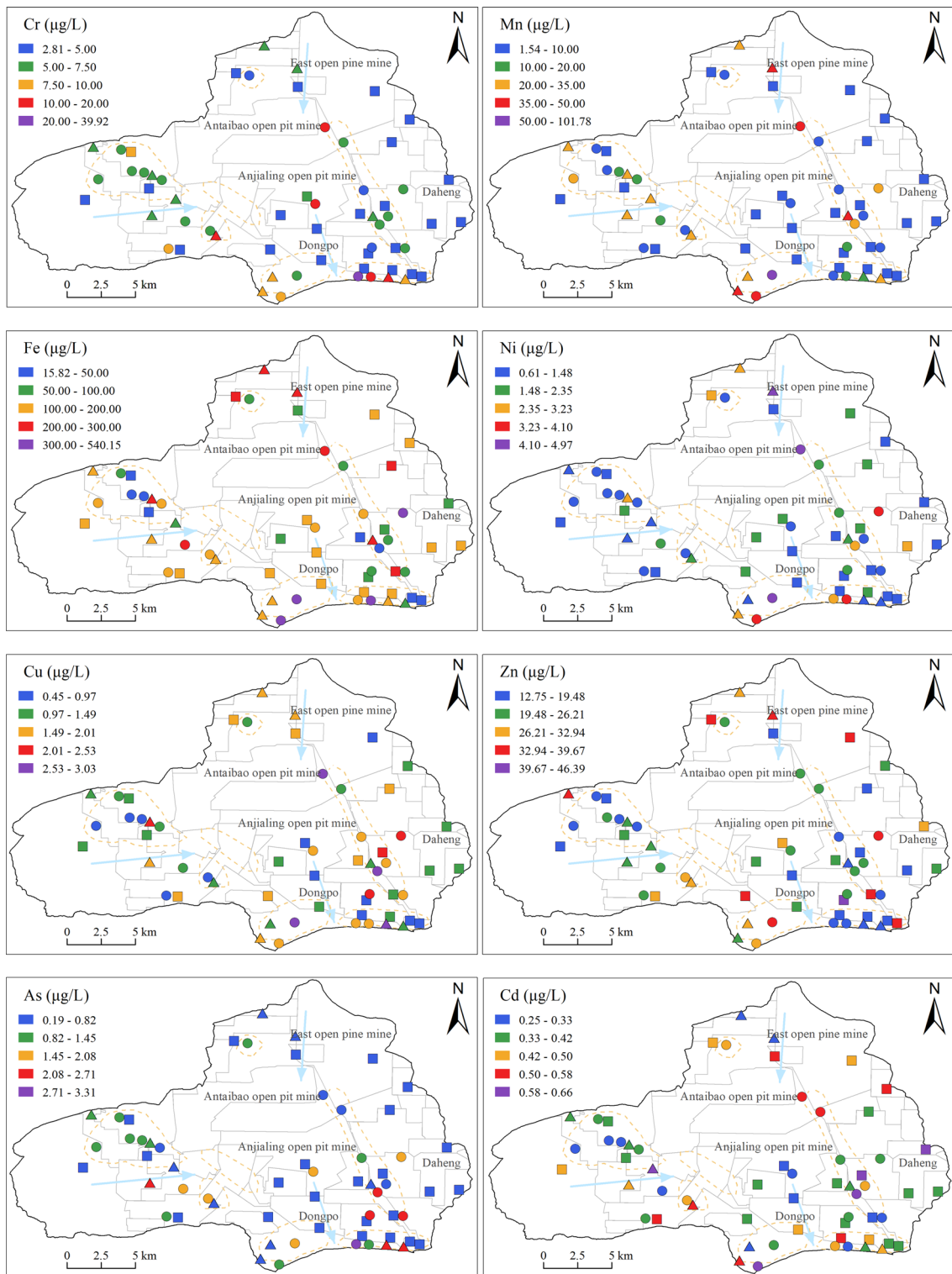


Fig. 3 Spatial distribution of HMs concentrations in groundwater in the study area

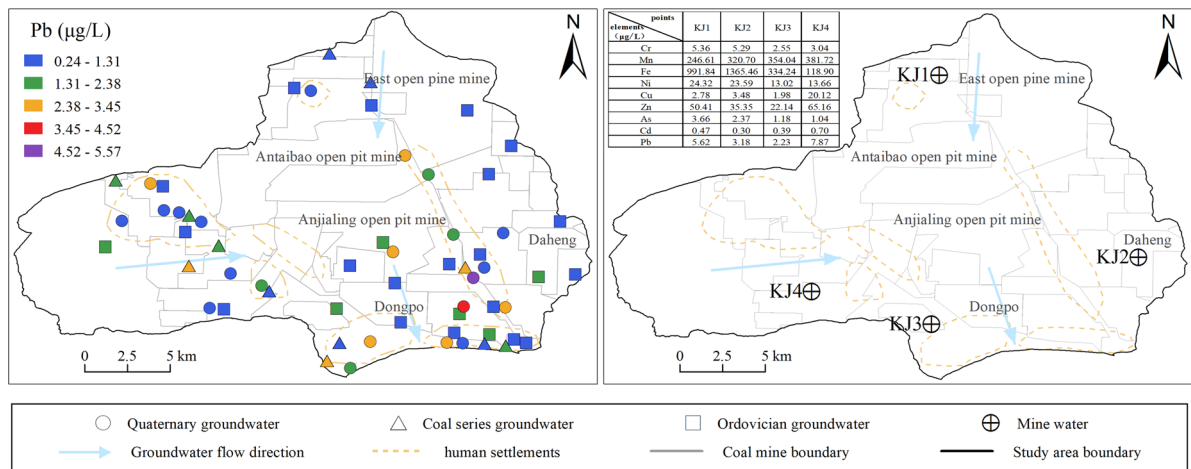


Fig. 3 (continued)

the credibility of results evaluation, and to make the conclusion more convincing (Kara et al., 2021). For example, a strong correlation between HMs in groundwater indicates that these elements have the same source or similar migration and transformation processes (Chai et al., 2021). Therefore, the Pearson correlation analysis between the concentration of HMs and pH in groundwater was conducted (Table 2) to explore the source and migration characteristics of HMs in groundwater in the Pingshuo mining area. The highly significant ($P < 0.001$) positive correlation between Fe, Ni, Cu, Zn, As, Pb, and Mn reveals that these HMs may have similar geochemical

behaviors or the same origins (Jiang et al., 2021b). The correlations between Mn and Fe or Ni, and the correlation between Zn and Pb or Cu were strongly significant ($r > 0.5$, $P < 0.001$), which reinforces the above conclusion. There was a significant ($P < 0.05$) negative relationship between Cr and Zn, and a significant ($P < 0.001$) positive relationship between Cr and As, indicating that the source of Cr in groundwater was more complex, partly homologous to Zn and partly homologous to As. The common behavior of Cr and As, as oxyanion species, can also explain this phenomenon. Ni was positively ($P < 0.001$) correlated with Cu, Zn, As, and Pb, indicating that Ni

Table 2 Pearson correlation matrix of pH and HMs in groundwater

	Cr	Mn	Fe	Ni	Cu	Zn	As	Cd	Pb	pH
Cr	1									
Mn	-0.079	1								
Fe	0.046	0.597***	1							
Ni	-0.007	0.837***	0.783***	1						
Cu	-0.036	0.392***	0.066	0.361***	1					
Zn	-0.147*	0.383***	0.286***	0.445***	0.625***	1				
As	0.438***	0.306***	0.419***	0.421***	0.083	0.066	1			
Cd	0.024	0.111	-0.067	0.092	0.341***	0.214**	0.013	1		
Pb	0.067	0.444***	0.282***	0.495***	0.763***	0.522***	0.441***	0.355***	1	
pH	0.301***	-0.043	0.082	-0.037	-0.084	0.049	0.233**	0.09	-0.038	1

*Correlation significant at the 0.01 level

**Correlation significant at the 0.005 level

***Correlation significant at the 0.001 level

in groundwater was partly originated from the same sources as Cu and Zn, and partly from the same sources as As and Pb. Zhou et al. (2019) showed that Zn, Cd, and Pb were chalcophile elements, having the same geochemical behavior. In the current study, Cu had significant positive correlation with Zn, Cd, and Pb, further explaining the homology of Cu with Zn, Cd, and Pb. In this study, the pH of groundwater was positively correlated with Cr ($P < 0.001$) and As ($P < 0.01$), which indicated that the acidity and alkalinity of groundwater affect the distribution of Cr and As concentrations, as well as the migration, transformation, and deposition enrichment of Cr and As in water. In agreement with our findings, Adeli et al. (2021) reported that with increase in pH value, the positive charge on rock and soil decreased, which decreased their As adsorption capacity, and increased the concentration of As in groundwater. Moreover, the relatively high pH can mobilize the adsorbed Cr into groundwater (Yan et al., 2022).

PMF model

Figure 4 shows the results of PMF model analysis on the origins of HMs in groundwater in Pingshuo mining area. The relative contributions of the factors for each sample were calculated using Eq. 4 (Yoon et al., 2023) and their averages in each type groundwater are

presented in Table 3. Among the factors, HMs with a high loading were used as the representative HMs of a certain source (Sheng et al., 2022). The PMF identified that three major sources contributed to the origin of HMs in groundwater. Factor 1 was the major contributor to the origin of HMs in groundwater, accounting for 68.22% of the total variance. The major contributors to Factor 1 score were Mn (96.57%), Fe (78.87%), and Ni (70.10%). Factor 1 mainly contributed to the origin of HMs in mine water (75.04%) and coal series groundwater (31.60%). Shanxi coal seam contains a large amount of pyrite, and coal mining makes the occurrence of pyrite reduction environment into an oxidizing environment, and thus water-rock interaction allows large amounts of Fe to seep into groundwater (Sun et al., 2022b). Ni is associated with coal seams in the form of sulfide and iron-manganese

Table 3 Relative contributions of factors for different types of groundwater based on PMF analysis results

Types	Contribution (%)		
	Factor 1	Factor 2	Factor 3
Quaternary groundwater	17.96	46.31	35.73
Coal series groundwater	31.60	39.23	29.17
Ordovician groundwater	13.98	31.57	54.45
Mine water	75.04	15.32	9.64

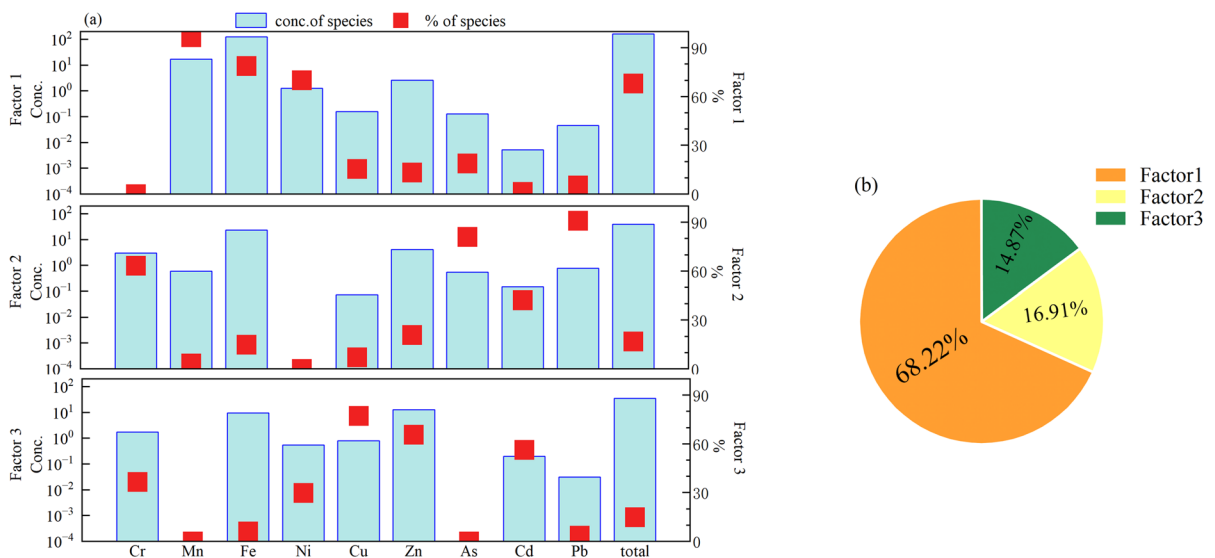


Fig. 4 The results of the PMF Model. **a** Contributions of three factors derived from the PMF model to the HMs. **b** Contribution of each factor

oxide, and the content of Ni in the leaching solution of coal and gangue is quite high (Chen et al., 2022). In coal resource exploitation, Ni, Fe, and Mn seep into groundwater (Bhuiyan et al., 2010; Wang et al., 2020). Kara et al. (2021) found that if groundwater contains Fe, it is very likely that Mn will also be present it. The results above showed that Mn, Fe, and Ni in groundwater in the study area were strongly associated with coal mining, as reflected by greater concentrations in coal series groundwater and mine water (Table 1). There was also a strong correlation of Ni, Fe, and Mn (Table 2). Therefore, Factor 1 was identified to be coal mining activities.

The contribution Factor 2 to the origin of HMs in groundwater in Pingshuo mining area was 16.91%. The prominently dominant HMs originating from Factor 2 were Pb (90.95%), As (81.01%), and Cr (63.38%), respectively. Sharma et al. (2022) showed that high concentrations of Pb in groundwater originated from anthropogenic sources such as vehicle emissions and agricultural chemical wastes. High Pb levels are also present in plastic filmland phosphate fertilizers (Wang et al., 2020). In this study, the higher concentration of Pb in mine water is mainly due to emissions from the large mining machinery and petroleum leakage during maintenance. The As is mainly produced by human activities. Agricultural activities such as chemical fertilizers and pesticides deposit As into the soil, and from the soil it leaches out into groundwater (Wang et al., 2019a). Human domestic sewage and poultry farms can cause an increase in Cr concentration in groundwater (Cai et al., 2019; Chen et al., 2022). Combined with the spatial distribution of Pb, As, and Cr in groundwater, the high-value area is mainly the area with strong human activity (Fig. 3). Hence, Factor 2 was identified to be representing HMs originating from the industrial, agricultural, and residential chemicals residues and leakages.

Factor 3 accounted for 14.87% of the total contribution to the origin of HMs in groundwater in Pingshuo mining area, which was distinguished by Cu (77.31%), Zn (65.68%), and Cd (56.28%). The Ordovician groundwater was predominantly affected by Factor 3 (54.45%). The concentration of Cu and Zn in the lower stratum is greater than that in the upper stratum (Ma et al., 2007). Many artificial landforms, such as waste piles, gangue piles, and dumps, have appeared on the surface of coal mining. The strata are also artificially inverted, exposing the lower strata

to the surface. A large amount of dust is produced during open-pit mining and transportation of coal mines, including pulverized coal particles, which settle downstream of the basin with wind transportation. These surface pollutants are prone to oxidation and contribute to HMs load of the soil, and during atmospheric precipitation, the HMs leach out into groundwater (Kim et al., 2023). In the spatial distribution, Cu and Ni had higher values in Quaternary groundwater, and were mostly concentrated near the dump and waste pile, and the downstream of the basin had more concentration of these HMs than the upstream. According to the previous analysis, the coefficient of variation of Cd is low, and the lithological changes of the strata caused the spatial differences. Cd is less affected by human activities and mainly affected by the geochemical background values. In addition to local interference by human factors, Cr and Zn are highly abundant, with relatively stable and uniform, overall spatial distribution, mainly affected by the geological background. Factor 3 was identified to be representing HMs originating derived from the geological dissolution of surface deposits, pollutant deposits, and water-bearing strata under the interaction of water and rock, which was identified as a natural source. The contribution of three factors to the enrichment of HMs in groundwater is shown in Fig. 4b. Factor 1 (coal mining activities), contributed the most (68.22%), followed by Factor 2 (industrial, agricultural and residential chemicals residue and leakage) which contributed 16.91%, and Factor 3 (natural source) contributed 14.87%. The PMF model factor scores clearly demonstrated that coal mining activities in the Pingshuo mining area were the most important contributor to the high level of heavy metals in groundwater.

Risk assessment of HMs in groundwater

HMs pollution assessment

The pollution index of the HMs in groundwater was assessed using the Nemerow pollution index (PI_N) (Sheng et al., 2022). The PI_N of each water sample was computed by referring HMs concentration data in the groundwater to the standard value of Class III of GB/T 14848–2017, followed by grade evaluation and proportion analysis (Table 4 and Fig. 5). Based on the water quality classification criteria of PI_N ,

approximately 15.15% and 7.58% of the samples for the Quaternary groundwater were classified as warn and mild HMs pollution, respectively, whereas 77.27% of the samples had no pollution. There was no pollution in coal series groundwater, and only 13.89% of samples caused the alert. Expectedly, there was no pollution in Ordovician groundwater. Contrary, the pollution of mine water was alarming, with 66.67 and 25.00% of the total water samples being in moderate and heavy pollution levels, respectively. As shown in Fig. 5, the total average value of the Nemerow pollution index in groundwater was greater for mine water, followed by Quaternary groundwater, coal series groundwater, and Ordovician groundwater in descending order. The same seasonal variation trend, low in stable and high in high-water periods, was also shown by Nemerow pollution index for the Quaternary groundwater and coal series groundwater. During the period of high–stable–low water, the Nemerow index was found to increase gradually in the Ordovician groundwater and mine water.

Health risk assessment

The health risks were assessed for adults and children considering ingestion and dermal absorption of groundwater-containing HMs in the research area. The results of non-carcinogenic evaluation are presented in Table 5, 67. No health risk assessment was performed for mine water, as there was no exposure to ingestion and dermal absorption. For adults and children, the HQ variation trend of HMs was consistent under the same exposure route to the same groundwater, while it was different in different exposure routes to different groundwater. Under the ingestion pathway, the average HQ of HMs in the Quaternary groundwater, coal series groundwater, and Ordovician groundwater followed a decreasing order as $As > Cr > Pb > Cd > Mn > Fe > Ni > Zn > Cu$, $As > Cr > Mn > Pb > Cd > Fe > Ni > Zn > Cu$, and $Cr > As > Cd > Pb > Mn > Fe > Zn > Ni > Cu$, respectively. The HQ of As in Quaternary groundwater and coal series groundwater was greater than that of Cr, while the opposite result was obtained in Ordovician groundwater. For Cd, Pb, and Mn, the HQ of

Table 4 Assessment results of Nemerow pollution index of HMs in groundwater of the study area (%)

Types	No pollution	Clean	Warn	Mild pollution	Moderate pollution	Heavy pollution
Quaternary groundwater	65.15	12.12	15.15	7.58	0	0
Coal series groundwater	69.44	16.67	13.89	0	0	0
Ordovician groundwater	86.67	13.33	0	0	0	0
Mine water	0	0	0	8.33	66.67	25.00

Fig. 5 Seasonal variation characteristics of the Nemerow pollution index

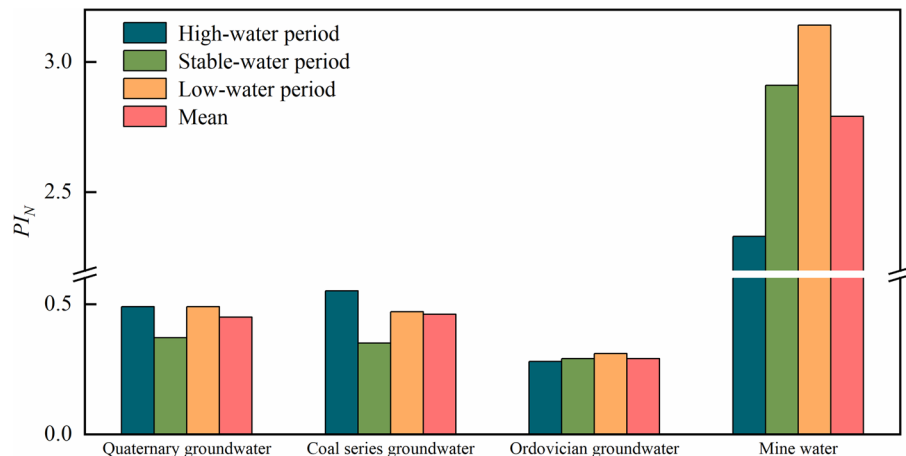


Table 5 Values of HQ (for each HM) for adults and children in groundwater through ingestion

Items	Quaternary groundwater		Coal series groundwater		Ordovician groundwater	
	adults	children	adults	children	adults	children
Cr	9.90×10^{-2}	1.31×10^{-1}	9.23×10^{-2}	1.22×10^{-1}	4.70×10^{-2}	6.24×10^{-2}
Mn	2.41×10^{-2}	3.19×10^{-2}	4.38×10^{-2}	5.80×10^{-2}	6.80×10^{-3}	9.02×10^{-3}
Fe	8.42×10^{-3}	1.12×10^{-2}	8.96×10^{-3}	1.19×10^{-2}	5.92×10^{-3}	7.85×10^{-3}
Ni	3.32×10^{-3}	4.41×10^{-3}	3.51×10^{-3}	4.66×10^{-3}	2.37×10^{-3}	3.15×10^{-3}
Cu	1.43×10^{-3}	1.90×10^{-3}	1.40×10^{-3}	1.86×10^{-3}	1.12×10^{-3}	1.49×10^{-3}
Zn	2.57×10^{-3}	3.41×10^{-3}	2.87×10^{-3}	3.81×10^{-3}	2.78×10^{-3}	3.69×10^{-3}
As	1.63×10^{-1}	2.17×10^{-1}	1.28×10^{-1}	1.70×10^{-1}	4.11×10^{-2}	5.45×10^{-2}
Cd	2.81×10^{-2}	3.73×10^{-2}	2.96×10^{-2}	3.92×10^{-2}	2.94×10^{-2}	3.90×10^{-2}
Pb	4.46×10^{-2}	5.92×10^{-2}	3.75×10^{-2}	4.97×10^{-2}	1.87×10^{-2}	2.48×10^{-2}
HQ _{ingestion}	3.75×10^{-1}	4.97×10^{-1}	3.48×10^{-1}	4.62×10^{-1}	1.55×10^{-1}	2.06×10^{-1}

Table 6 Values of HQ (for each HM) for adults and children in groundwater through dermal absorption

Items	Quaternary groundwater		Coal series groundwater		Ordovician groundwater	
	adults	children	adults	children	adults	children
Cr	3.55×10^{-2}	7.37×10^{-2}	3.31×10^{-2}	6.87×10^{-2}	1.69×10^{-2}	3.50×10^{-2}
Mn	2.70×10^{-3}	5.60×10^{-3}	4.90×10^{-3}	1.02×10^{-2}	7.62×10^{-4}	1.58×10^{-3}
Fe	1.89×10^{-4}	3.92×10^{-4}	2.01×10^{-4}	4.17×10^{-4}	1.33×10^{-4}	2.75×10^{-4}
Ni	7.45×10^{-5}	1.55×10^{-4}	7.87×10^{-5}	1.63×10^{-4}	5.32×10^{-5}	1.10×10^{-4}
Cu	3.21×10^{-5}	6.66×10^{-5}	3.14×10^{-5}	6.52×10^{-5}	2.51×10^{-5}	5.22×10^{-5}
Zn	3.45×10^{-5}	7.18×10^{-5}	3.86×10^{-5}	8.02×10^{-5}	3.74×10^{-5}	7.77×10^{-5}
As	7.71×10^{-4}	1.60×10^{-3}	6.05×10^{-4}	1.26×10^{-3}	1.94×10^{-4}	4.03×10^{-4}
Cd	2.52×10^{-3}	5.24×10^{-3}	2.65×10^{-3}	5.50×10^{-3}	2.64×10^{-3}	5.48×10^{-3}
Pb	6.66×10^{-5}	1.38×10^{-4}	5.60×10^{-5}	1.16×10^{-4}	2.79×10^{-5}	5.79×10^{-5}
HQ _{dermal}	4.19×10^{-2}	8.70×10^{-2}	4.17×10^{-2}	8.65×10^{-2}	2.07×10^{-2}	4.31×10^{-2}

Table 7 Values of HI for adults and children in groundwater

Items	Quaternary groundwater		Coal series groundwater		Ordovician groundwater	
	adults	children	adults	children	adults	children
HI	0.42	0.58	0.39	0.55	0.18	0.25

Pb, Mn, and Cd was higher than the other elements in Quaternary groundwater, coal series groundwater, and Ordovician groundwater, respectively. Fe, Ni, Zn, and Cu ranked the last four in each type of groundwater. Under the dermal absorption pathway, the HQ of HMs for Quaternary groundwater and coal series groundwater in descending order was Cr > Mn > Cd > As > Fe > Ni > Pb > Zn > Cu, while for Ordovician groundwater: Cr > Cd > Mn > As > Fe > Ni > Zn > Pb > Cu. The HQ of Mn in Quaternary groundwater and coal series groundwater was 10 times greater than that in Ordovician groundwater, thus indicating that

Mn has a serious impact on these two aquifers (Shi et al., 2022). The non-carcinogenic total health risk quotient in children was significantly greater than in adults. Moreover, ingestion was greater than dermal absorption. The total health risk quotient of ingestion was about seven to nine times greater than that of dermal absorption in adults and four to six times greater than that of ingestion in children.

As shown in Table 7, the non-carcinogenic health risk index (HI) of HMs in groundwater ranged from 0.18 to 0.42 for adults and 0.25 to 0.58 for children, all were within acceptable (< 1) range. The HI

of HMs for groundwater in descending order was Quaternary groundwater > coal series groundwater > Ordovician groundwater. The HI of Ordovician groundwater was the lowest, 0.43 to 0.46 times that of other water bodies. The HI of children was 1.34 to 1.41 times higher than that of adults, indicating that HMs pollution in groundwater in the Pingshuo mining area posed a higher non-carcinogenic health risk to children (Wen et al., 2019).

Chronic consumption or exposure to water contaminated with HMs poses a health hazard to the human body and even causes cancer (Sajjadi et al., 2022). In this study, all carcinogenic HMs (Cr, As, and Cd) in groundwater were modeled to estimate incremental lifetime cancer risk (ILCR) in the research area. The carcinogenic risk assessment results of HMs in groundwater through ingestion and dermal absorption are shown in Fig. 6. The carcinogenic risk value of HMs in groundwater > 1×10^{-4} indicated high carcinogenic risk; 1×10^{-6} to 1×10^{-4} represented an admissible range, and $< 1 \times 10^{-6}$ indicated negligible risk (Li et al., 2022). For adults and children, 65.15 and 81.82% of Quaternary groundwater, 80.56 and 83.33% of coal series groundwater, 6.67 and 17.33% of Ordovician groundwater pose a high carcinogenic risk of Cr, and the rest were within the admissible limit of carcinogenic risk. For adults and children, 28.79 and 37.88% of Quaternary groundwater, 19.44

and 25.00% of coal series groundwater pose a high carcinogenic risk of As, whereas Ordovician groundwater was within the acceptable range of carcinogenic risk. The carcinogenic risk of Cd in all groundwater was low. Cr and As had the greatest impact on the health carcinogenic risk of adults and children, followed by Cd. The lower (about 1–2 orders of magnitude) carcinogenic risk of HMs in groundwater occurred through dermal absorption compared to through ingestion. As shown in Fig. 6c, d, the carcinogenic risk of dermal absorption to Cr, As, and Cd in adults and children in all groundwater was acceptable or negligible. Furthermore, the carcinogenic risk of HMs through ingestion and dermal absorption has been reported to be higher in children than in adults (Zhong et al., 2022).

The total carcinogenic risk value of groundwater in each type of groundwater was obtained by adding the calculated carcinogenic risk values of HMs from ingestion and dermal absorption. According to the calculation results, for children, 100% of Quaternary groundwater, 94.44% of coal series groundwater, and 90.67% of Ordovician groundwater had high carcinogenic risks; for adults, 95.45% of Quaternary groundwater, 91.67% of coal series groundwater, and 26.67% of Ordovician groundwater had high carcinogenic risks. This revealed that children in the research area were more sensitive to the threat

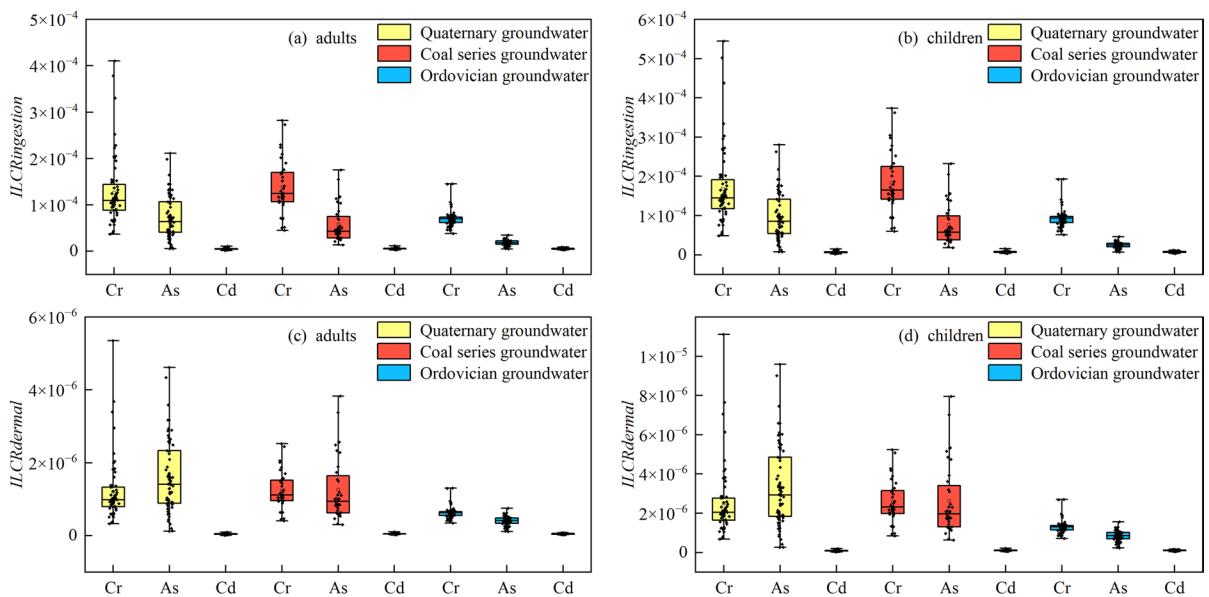


Fig. 6 Carcinogenic health risk value for adults and children in groundwater through ingestion and dermal absorption

of HM carcinogenesis in groundwater. The Quaternary and coal series groundwater resulted unsuitable for drinking and use as domestic water. The Ordovician groundwater also posed a high carcinogenic risk due to the pollution of human activities such as coal mining. In the future, it should be well protected and should be taken certain purification measures as far as possible before use.

Conclusions

This study systematically evaluated the concentrations, spatiotemporal distribution characteristics, and contamination sources, and pollution and health risks of HMs in groundwater in Pingshuo coal mining area. The results showed that Fe, Mn, and Zn had the highest concentrations across various types of groundwater. The concentrations of HMs were higher in groundwater near the open pit, waste slag pile, riverfront area, and high anthropic zone. Except for Ordovician groundwater, excessive HMs were found in all investigated groundwater of the mining area, as compared with the standard thresholds. Fe exceeded the threshold in 13% to 75% of the groundwater sampled. Most HMs concentrations of Quaternary groundwater, Ordovician groundwater, and mine water in the low-water period are higher than those in stable and high period, while the higher HMs concentration of coal series groundwater in the high-water period were observed. Three sources of HMs in groundwater were identified and quantified by PMF model, including coal mining activities (Factor 1, 68.22%), industrial, agricultural, and residential chemicals residue and leakage (Factor 2, 16.91%), and natural sources (Factor 3, 14.87%). The Quaternary groundwater, Ordovician groundwater, and mine water were mainly affected by Factor 2, Factor 3, and Factor 1, respectively. The coal series groundwater was affected by the combination of all three factors. The Nemerow pollution index revealed that 7.58 and 100% of Quaternary groundwater and mine water samples were polluted. The health risk index for HMs in groundwater showed that the non-carcinogenic health risk ranged from 0.18 to 0.42 for adults, indicating an acceptable level. Additionally, high carcinogenic risks were identified in Quaternary groundwater

(95.45%), coal series groundwater (91.67%), and Ordovician groundwater (26.67%). Both carcinogenic and non-carcinogenic risks were greater for children than adults, highlighting their increased vulnerability to HMs in groundwater. Cr and As had the greatest impact on the health carcinogenic risk of adults and children, followed by Cd. Therefore, the groundwater in the study area should be well protected, and certain purification measures should be taken before use.

Acknowledgements The authors are grateful to the anonymous reviewers and the editors for their valuable suggestions and comments on the manuscript. We thank Mr. Guanghua Liu, Ms. Lin Sun and Ms. Meng He for the assistant of the sample pretreatment and index test.

Author contributions LS was involved in data collection, formal analysis, investigation, software, writing—original draft, writing—review & editing. TL helped in supervision, project administration, funding acquisition. LD assisted in reviewing, project administration. XT, WZ, HC, ZW, and GZ helped in investigation.

Funding This work was supported by the National Natural Science Foundation of China (The Yellow River Water Science Research Joint Found U2243234), the National Natural Science Foundation of China (No. 51939006), the Inner Mongolia Autonomous Region Science and Technology Leading Talent Team (No. 2022LJRC0007), the Ministry of Education Innovative Research Team (No. IRT_17R60), the Science and Technology Innovation Team in Key fields of Ministry of Science and Technology, China (No. 2015RA4013), the Inner Mongolia Industrial Innovative Research Team (2012), the Inner Mongolia Agricultural University Basic Research Project (Nos. BR221204 and BR221012).

Data availability The datasets used or analyzed during the current study are available from the corresponding author on reasonable request.

Declarations

Conflict of interest The authors have no conflicts of interest to declare that are relevant to the content of this article.

Consent to participate Consent for publication was obtained from all participants.

References

- Adeli, M., Mohammadi, Z., Keshavarzi, B., Amjadian, K., & Kafi, M. (2021). Heavy metal(loid) pollution of a hard-rock aquifer: Evidence, distribution, and source. *Environmental Science and Pollution*

- Research*, 28(26), 34742–34761. <https://doi.org/10.1007/s11356-021-13079-2>
- Ali, H., Khan, E., & Sajad, M. A. (2013). Phytoremediation of heavy metals-concepts and applications. *Chemosphere*, 91(7), 869–881. <https://doi.org/10.1016/j.chemosphere.2013.01.075>
- Bhuiyan, M. A. H., Parvez, L., Islam, M. A., Dampare, S. B., & Suzuki, S. (2010). Heavy metal pollution of coal mine-affected agricultural soils in the northern part of Bangladesh. *Journal of Hazardous Materials*, 173(1–3), 384–392. <https://doi.org/10.1016/j.jhazmat.2009.08.085>
- Bodrud-Doza, M., Bhuiyan, M. A. H., Islam, S. M. D., Qurashi, S. B., Muhib, M. I., Rakib, M. A., & Rahman, M. S. (2019). Delineation of trace metals contamination in groundwater using geostatistical techniques: a study on Dhaka City of Bangladesh. *Groundwater for Sustainable Development*. <https://doi.org/10.1016/j.gsd.2019.03.006>
- Caboi, R., & Cidu, R. (1999). Environmental mineralogy and geochemistry of the abandoned Pb-Zn montevecchio-Ingurto mining district, Sardinia, Italy. *Chronique De La Recherche Miniere*, 67, 21–28.
- Cai, L. M., Wang, Q. S., Wen, H. H., Luo, J., & Wang, S. (2019). Heavy metals in agricultural soils from a typical township in Guangdong province, China: Occurrences and spatial distribution. *Ecotoxicology and Environmental Safety*, 168, 184–191. <https://doi.org/10.1016/j.ecoenv.2018.10.092>
- Chai, L., Wang, Y. H., Wang, X., Ma, L., Cheng, Z. X., & Su, L. M. (2021). Pollution characteristics, spatial distributions, and source apportionment of heavy metals in cultivated soil in Lanzhou, China. *Ecological Indicators*, 125, 107507. <https://doi.org/10.1016/j.ecolind.2021.107507>
- Chen, J. Y., Gui, H. R., Guo, Y., & Li, J. (2022). Health risk assessment of heavy metals in shallow groundwater of coal-poultry farming districts. *International Journal of Environmental Research and Public Health*, 19(19), 12000. <https://doi.org/10.3390/ijerph191912000>
- Cui, L., Wang, X. N., Li, J., Gao, X. Y., Zhang, J. W., & Liu, Z. T. (2021). Ecological and health risk assessments and water quality criteria of heavy metals in the Haihe river. *Environmental Pollution*, 290, 117971. <https://doi.org/10.1016/j.envpol.2021.117971>
- Egbueri, J. C., & Unigwe, C. O. (2020). Understanding the extent of heavy metal pollution in drinking water supplies from Umunya, Nigeria: An indexical and statistical assessment. *Analytical Letters*, 53(13), 2122–2144. <https://doi.org/10.1080/00032719.2020.1731521>
- Giri, S., & Singh, A. K. (2014). Risk assessment, statistical source identification and seasonal fluctuation of dissolved metals in the Subarnarekha River, India. *Journal of Hazardous Materials*, 265, 305–314. <https://doi.org/10.1016/j.jhazmat.2013.09.067>
- Gu, C. K., Zhang, Y., Peng, Y., Leng, P. F., Zhu, N., Qiao, Y. F., Li, Z., & Li, F. D. (2020). Spatial distribution and health risk assessment of dissolved trace elements in groundwater in southern China. *Scientific Reports*, 10(1), 7886. <https://doi.org/10.1038/s41598-020-64267-y>
- Guo, Y., Zhang, Y. X., Zhao, X., Xu, J., Qiu, G. F., Jia, W. K., Wu, J. J., & Guo, F. H. (2022). Multifaceted evaluation of distribution, occurrence, and leaching features of typical heavy metals in different-sized coal gasification fine slag from Ningdong region, China: A case study. *Science of the Total Environment*, 831, 154726. <https://doi.org/10.1016/j.scitotenv.2022.154726>
- Haghnazar, H., Johannesson, K. H., Gonzalez-Pinzon, R., Pourakbar, M., Aghayani, E., Rajabi, A., & Hashemi, A. A. (2022). Groundwater geochemistry, quality, and pollution of the largest lake basin in the Middle East: Comparison of PMF and PCA-MLR receptor models and application of the source-oriented HHRA approach. *Chemosphere*, 288(1), 132489. <https://doi.org/10.1016/j.chemosphere.2021.132489>
- Haque, M. M., Niloy, N. M., Nayna, O. K., Fatema, K. J., Qurashi, S. B., Park, J., Kim, K., & Tareq, S. M. (2020). Variability of water quality and metal pollution index in the Ganges River, Bangladesh. *Environmental Science and Pollution Research*, 27(34), 42582–42599. <https://doi.org/10.1007/s11356-020-10060-3>
- Huang, J. L., Wu, Y. Y., Sun, J. X., Li, X., Geng, X. L., Zhao, M. L., Sun, T., & Fan, Z. Q. (2021). Health risk assessment of heavy metal(loid)s in park soils of the largest megacity in China by using Monte Carlo simulation coupled with positive matrix factorization model. *Journal of Hazardous Materials*, 415, 125629. <https://doi.org/10.1016/j.jhazmat.2021.125629>
- Jiang, C. L., Zhao, Q., Zheng, L. G., Chen, X., Li, C., & Ren, M. X. (2021a). Distribution, source and health risk assessment based on the monte carlo method of heavy metals in shallow groundwater in an area affected by mining activities, China. *Ecotoxicology and Environmental Safety*, 224(112679), 112679. <https://doi.org/10.1016/j.ecoenv.2021.112679>
- Jiang, H. H., Cai, L. M., Hu, G. C., Wen, H. H., Luo, J., Xu, H. Q., & Chen, L. G. (2021b). An integrated exploration on health risk assessment quantification of potentially hazardous elements in soils from the perspective of sources. *Ecotoxicology and Environmental Safety*, 208, 111489. <https://doi.org/10.1016/j.ecoenv.2020.111489>
- Kara, H., Yetis, A. D., & Temel, H. (2021). Assessment of heavy metal contamination in groundwater of Diyarbakir oil production area, (Turkey) using pollution indices and chemometric analysis. *Environmental Earth Sciences*, 80(20), 697–711. <https://doi.org/10.1007/s12665-021-10011-2>
- Kaur, M., Kumar, A., Mehra, R., & Kaur, I. (2020). Quantitative assessment of exposure of heavy metals in groundwater and soil on human health in Reasi district, Jammu and Kashmir. *Environmental Geochemistry and Health*, 42(1), 77–94. <https://doi.org/10.1007/s10653-019-00294-7>
- Khan, R., Saxena, A., & Shukla, S. (2021). Assessment of the impact of COVID-19 lockdown on the heavy metal pollution in the River Gomti, Lucknow city, Uttar Pradesh, India. *Environmental Quality Management*. <https://doi.org/10.1002/tqem.21746>
- Kim, D. M., Kwon, H. L., & Im, D. G. (2023). Determination of contamination sources and geochemical behaviors of metals in soil of a mine area using Cu, Pb, Zn, and S isotopes and positive matrix factorization. *Journal of Hazardous Materials*, 447, 130827. <https://doi.org/10.1016/j.jhazmat.2023.130827>
- Kim, D. M., Yun, S. T., Cho, Y., Hong, J. H., Batsaikhan, B., & Oh, J. (2017). Hydrochemical assessment of

- environmental status of surface and ground water in mine areas in South Korea: Emphasis on geochemical behaviors of metals and sulfate in ground water. *Journal of Geochemical Exploration*, 183, 33–45. <https://doi.org/10.1016/j.gexplo.2017.09.014>
- Li, L. M., Wu, J., Lu, J., Li, K. X., Zhang, X. Y., Min, X. Y., Gao, C. L., & Xu, J. (2022). Water quality evaluation and ecological-health risk assessment on trace elements in surface water of the northeastern Qinghai-Tibet Plateau. *Ecotoxicology and Environmental Safety*, 241, 113775. <https://doi.org/10.1016/j.ecoenv.2022.113775>
- Liu, J., Liu, Y. J., Liu, Y., Liu, Z., & Zhang, A. N. (2018). Quantitative contributions of the major sources of heavy metals in soils to ecosystem and human health risks: A case study of Yulin, China. *Ecotoxicology and Environmental Safety*, 164, 261–269. <https://doi.org/10.1016/j.ecoenv.2018.08.030>
- Ma, C. A., Wang, Q. R., & Cai, Q. X. (2007). Evaluation of heavy metal pollution in large open-pit coal mines. *Mining Safety and Environmental Protection*, 34(2), 36–40.
- Mahapatra, S. R., Venugopal, T., Shanmugasundaram, A., Giridharan, L., & Jayaprakash, M. (2020). Heavy metal index and geographical information system (GIS) approach to study heavy metal contamination: A case study of north Chennai groundwater. *Applied Water Science*, 10(12), 1–17. <https://doi.org/10.1007/s13201-020-01321-0>
- Miguel, D. E., Iribarren, I., Chacón, E., Ordoñez, A., & Charlesworth, S. (2007). Risk-based evaluation of the exposure of children to trace elements in playgrounds in Madrid (Spain). *Chemosphere*, 66(3), 505–513. <https://doi.org/10.1016/j.chemosphere.2006.05.065>
- Mukherjee, I., Singh, U. K., Singh, R. P., Anshumali, A., & KumariJhaMehta, D. P. K. P. (2020). Characterization of heavy metal pollution in an anthropogenically and geologically influenced semi-arid region of east India and assessment of ecological and human health risks. *Science of the Total Environment*, 705, 135801. <https://doi.org/10.1016/j.scitotenv.2019.135801>
- Qin, W. J., Han, D. G., Song, X. F., & Liu, S. H. (2021). Sources and migration of heavy metals in a karst water system under the threats of an abandoned Pb-Zn mine, Southwest China. *Environmental Pollution*, 277, 116774. <https://doi.org/10.1016/j.envpol.2021.116774>
- Qu, L. Y., Huang, H., Xia, F., Liu, Y. Y., Dahlgren, R. A., Zhang, M. H., & Mei, K. (2018). Risk analysis of heavy metal concentration in surface waters across the rural-urban interface of the Wen-Rui Tang River, China. *Environmental Pollution*, 237, 639–649. <https://doi.org/10.1016/j.envpol.2018.02.020>
- Sajjadi, S. A., Mohammadi, A., Khosravi, R., & Zarei, A. (2022). Distribution, exposure, and human health risk analysis of heavy metals in drinking groundwater of Ghayen County, Iran. *Geocarto International*, 37(26), 13127–13144. <https://doi.org/10.1080/10106049.2022.2076916>
- Santana, C. S., Olivares, D. M. M., Silva, V. H. C., Luzardo, F. H. M., Velasco, F. G., & Jesus, R. M. (2020). Assessment of water resources pollution associated with mining activity in a semi-arid region. *Journal of Environmental Management*. <https://doi.org/10.1016/j.jenvman.2020.111148>
- Sharma, K., Raju, N. J., Singh, N., & Sreekes, S. (2022). Heavy metal pollution in groundwater of urban Delhi environs: Pollution indices and health risk assessment. *Urban Climate*. <https://doi.org/10.1016/j.uclim.2022.101233>
- Sheng, D. R., Meng, X. H., Wen, X. H., Wu, J., Yu, H. J., & Wu, M. (2022). Contamination characteristics, source identification, and source-specific health risks of heavy metal(loid)s in groundwater of an arid oasis region in Northwest China. *Science of the Total Environment*, 841, 156733. <https://doi.org/10.1016/j.scitotenv.2022.156733>
- Shi, X. M., Liu, S., Song, L., Wu, C. S., Yang, B., Lu, H. Z., Wang, X., & Zakari, S. (2022). Contamination and source-specific risk analysis of soil heavy metals in a typical coal industrial city, central China. *Science of the Total Environment*, 836, 155694. <https://doi.org/10.1016/j.scitotenv.2022.155694>
- Shil, S., & Singh, U. K. (2019). Health risk assessment and spatial variations of dissolved heavy metals and metalloids in a tropical river basin system. *Ecological Indicators*, 106, 105455. <https://doi.org/10.1016/j.ecolind.2019.105455>
- Singh, U. K., & Kumar, B. (2017). Pathways of heavy metals contamination and associated human health risk in Ajay River basin, India. *Chemosphere*, 174, 183–199. <https://doi.org/10.1016/j.chemosphere.2017.01.103>
- Sun, L., Liu, T. X., Duan, L. M., Zhang, W. R., & Zheng, G. F. (2022a). Spatial and temporal characteristics of isotopes of different water sources and implications for water circulation in mining areas. *Advances in Water Science*, 33(5), 805–815. <https://doi.org/10.14042/j.cnki.32.1309.2022.05.010>
- Sun, L., Liu, T. X., Duan, L. M., Zhang, W. R., & Zheng, G. F. (2022b). Hydrochemical characteristics and fluorine distribution and causes of different water bodies in Pingshuo mining area. *Environmental Science*, 43(12), 5547–5559. <https://doi.org/10.13227/j.hjcx.202202176>
- Sun, S., Tang, Q. H., Konar, M., Huang, Z. W., Gleeson, T., Ma, T., Fang, C. L., & Cai, X. M. (2022c). Domestic groundwater depletion supports China's full supply chains. *Water Resources Research*, 58(5), e2021WR030695. <https://doi.org/10.1029/2021WR030695>
- Wang, F. F., Guan, Q. Y., Tian, J., Lin, J. K., Yang, Y. Y., Yang, L. Q., & Pan, N. H. (2020). Contamination characteristics, source apportionment, and health risk assessment of heavy metals in agricultural soil in the Hexi corridor. *CATENA*, 191, 104573. <https://doi.org/10.1016/j.catena.2020.104573>
- Wang, J., Liu, G. J., Liu, H. Q., & Lam, P. K. S. (2017). Multivariate statistical evaluation of dissolved trace elements and a water quality assessment in the middle reaches of Huaihe river, Anhui China. *Science of the Total Environment*, 583(1), 421–431. <https://doi.org/10.1016/j.scitotenv.2017.01.088>
- Wang, S., Cai, L. M., Wen, H. H., Luo, J., Wang, Q. S., & Liu, X. (2019a). Spatial distribution and source apportionment of heavy metals in soil from a typical county-level city of Guangdong Province, China. *Science of the Total*

- Environment*, 655(1), 92–101. <https://doi.org/10.1016/j.scitotenv.2018.11.244>
- Wang, Y., Jiao, J. J., Zhang, K., & Zhou, Y. Z. (2016). Enrichment and mechanisms of heavy metal mobility in a coastal quaternary groundwater system of the Pearl River Delta, China. *Science of the Total Environment*, 545–546, 493–502. <https://doi.org/10.1016/j.scitotenv.2015.12.019>
- Wang, Y., Dong, R., Zhou, Y. Z., & Luo, X. (2019b). Characteristics of groundwater discharge to river and related heavy metal transportation in a mountain mining area of Dabaoshan, Southern China. *Science of the Total Environment*, 679, 346–358. <https://doi.org/10.1016/j.scitotenv.2019.04.273>
- Wang, Z. Y., Su, Q., Wang, S., Gao, Z. J., & Liu, J. T. (2021). Spatial distribution and health risk assessment of dissolved heavy metals in groundwater of eastern China coastal zone. *Environmental Pollution*, 290, 118016. <https://doi.org/10.1016/j.envpol.2021.118016>
- Wen, X. H., Lu, J., Wu, J., Lin, Y. C., & Luo, Y. M. (2019). Influence of coastal groundwater salinization on the distribution and risks of heavy metals. *Science of the Total Environment*, 652, 267–277. <https://doi.org/10.1016/j.scitotenv.2018.10.250>
- Xiao, L. L., Li, W., Zhu, C. M., Yang, S. J., Zhou, M., Wang, B., Wang, X., Wang, D. M., Ma, J. X., Zhou, Y., & Chen, W. H. (2021). Cadmium exposure, fasting blood glucose changes, and type 2 diabetes mellitus: A longitudinal prospective study in China. *Environmental Research*, 192, 110259. <https://doi.org/10.1016/j.envres.2020.110259>
- Xie, H., Liang, Y. P., Li, J., Zou, S. Z., Shen, H. Y., Zhao, C. H., & Wang, Z. H. (2021). Distribution characteristics and health risk assessment of metal elements in groundwater of Longzici spring area. *Environmental Science*, 42(9), 4257–4266. <https://doi.org/10.13227/j.hjcx.202101204>
- Yan, D. X., Bai, Z. K., & Liu, X. Y. (2020). Heavy metal pollution characteristics and influencing factors in agricultural soils: Evidence from Shuozhou city, Shanxi province, China. *Sustainability*, 12(5), 1907–1921. <https://doi.org/10.3390/su12051907>
- Yan, S., Guo, H. M., Yin, J. H., Hu, H. Y., Cui, D., & Gao, B. Y. (2022). Genesis of high hexavalent chromium groundwater in deep aquifers from loess plateau of Northern Shaanxi, China. *Water Research*, 216, 118323. <https://doi.org/10.1016/j.watres.2022.118323>
- Yoon, S., Kim, D. M., Yu, S., Park, J., & Yun, S. T. (2023). Metal(loid)-specific sources and distribution mechanisms of riverside soil contamination near an abandoned gold mine in Mongolia. *Journal of Hazardous Materials*, 443, 130294. <https://doi.org/10.1016/j.jhazmat.2022.130294>
- Zhang, S. Z., Liu, G. J., & Yuan, Z. J. (2019). Environmental geochemistry of heavy metals in the groundwater of coal mining areas: A case study in Dingji coal mine, Huainan coalfield, China. *Environmental Forensics*, 20(3), 265–274. <https://doi.org/10.1080/15275922.2019.1629128>
- Zheng, C. M., & Bennett, G. D. (2002). *Applied contaminant transport modeling*. Wiley-Interscience.
- Zhong, C. H., Yang, Q. C., Liang, J., & Ma, H. Y. (2022). Fuzzy comprehensive evaluation with AHP and entropy methods and health risk assessment of groundwater in Yinchuan Basin, northwest China. *Environmental Research*, 204, 111956. <https://doi.org/10.1016/j.envres.2021.111956>
- Zhou, J. M., Jiang, Z. C., Xu, G. L., Qin, X. Q., Huang, Q. B., & Zhang, L. K. (2019). Water quality analysis and health risk assessment for groundwater at Xiangshui, Chongzuo. *Environmental Science*, 40(6), 2675–2685. <https://doi.org/10.13227/j.hjcx.201810234>

Publisher's Note Springer Nature remains neutral with regard to jurisdictional claims in published maps and institutional affiliations.

Springer Nature or its licensor (e.g. a society or other partner) holds exclusive rights to this article under a publishing agreement with the author(s) or other rightsholder(s); author self-archiving of the accepted manuscript version of this article is solely governed by the terms of such publishing agreement and applicable law.